Semester Learning Project

Autumn Semester, 2022, IIT Bombay

Polarization correlation of annihilation photons in Positron Emission Tomography

Rehmat Singh Chawla
200260039

November, 2022

Contents

Chapter 1

Abstract

Medical imaging is a subject of undeniable importance. It forms a crucial component of the non-invasive diagnostic procedures available in modern medicine. Thus, improving the quality of images while simultaneously trying to improve the safety of these procedures is the focus of a large body of research. In this project, I focus on one of the two broad categories of Nuclear Medical Imaging, PET scans, and attempt to understand how to improve their image quality using previously unexploited properties of the process causing the radiation.

Nuclear Medical Imaging takes advantage of the radioactive properties of certain materials and our ability to detect this radiation with high sensitivity. A radioactive material is injected into the body to be imaged, and detectors measure the radiation at different positions and angles. Then the source distribution is mathematically reconstructed. PET scans use a specific kind of radiation, annhilation photons. These are emitted in pairs, and hence they have various correlations in their properties, notably in their polarisations. I attempt to use this information to better identify true pairs from the detected photons and hence improve image quality.

Chapter 2

Theory

[3] has been referenced for a significant portion of this part of the project.

2.1 Nuclear Medical Imaging

The process of Nuclear Imaging generally consists of injecting radioactive materials into the body which is to be imaged, detecting the resulting radiation, and constructing an image from the data. The injected material is known as the *radio-pharmaceutical* (alternatively tracer or radiotracer). It relies on the preferential take-up of different radioactive materials by different organs or parts of the body, hence different radiotracers need to be used for imaging of different body parts.

Due to the permeability of gamma rays over alpha or beta rays through organic material, along with the comparitive safety, research has focused on medical imaging by detecting photons. This allows us to divide medical imaging into two broad categories:

Single Photon Imaging consists of radiotracers which emit a single photon in a decay event which is then detected.

The source event's position cannot generally be located precisely, but this is still effective for planar imaging, where detection is performed from one angle and depth information is lost. However, it is also possible to reconstruct a full image by collecting data from many an-

gles, which is known as *single photon emission computed tomography (SPECT)*.

Positron Imaging consists of radiotracers which decay by $\beta+$ or *positron* emission. These positrons annihilate with an electron to create two high-energy photons with almost equal and opposite momenta, and other properties such as polarisation also being correlated. This is immensely useful for localisation of the decay event, and can hence lead to better imaging. The subcategory of image reconstruction by taking data from multiple angles is known as *Positron Emission Tomography (PET)*.

2.2 Radioactive Decay Processes

The difference between Single Photon and Positron Imaging is perhaps the most striking example of how different types of decay processes can impact the efficiency of the imaging procedure. It is instructive to more thoroughly cover the types of decay processes a nucleus can commonly undergo.

Prior to that, some terminology needs to be introduced. An *nuclide* is an atom with a specific atomic number, mass number, energy state and the the arrangement of nucleons in the nucleus. We refer to unstable nuclides that may undergo radioactive decay as *radionuclides*. The decay process will lead to some loss of energy - this energy appears as a mass deficit between the final product and initial state, i.e. the mass converted to the energy. The total amount is known as the *transition energy* Q, and it is distributed among emitted photons, released particles, and the kinetic energy of the nucleus (though the latter is generally small). It is necessary to consider the energy at which one expects to detect photons, to optimise for the same.

The most stable state of a nucleus, the most stable arrangement of nucleons, is known as the *ground state*. Higher energy states can be categorised as

Excited states which are highly unstable arrangements and decay to some other state very quickly, and

Metastable states which are more stable and have relatively long lifetimes. The time period considered to be the dividing line between these two is $\sim 10^{-12}$ seconds. Some metastable states have long enough lifetimes

to be considered different nuclides altogether.

The notation used for a nuclide is ${}^{\mathrm{A(m)}}_{\mathrm{Z}}\mathrm{X}_{\mathrm{N}}{}^{(*)}$, where $m, *$ are optional and denote a metastable state and an excited state respectively. N, the number of neutrons, is often omitted, and since the element X uniquely determines the atomic number Z, that is often omitted too.

2.2.1 Characteristic Radiation

We will consider the Bohr model to be sufficiently accurate for the purposes of this section. In the Bohr model, the atom has various "shells" - various energy levels - which the electrons can occupy. There is a limited occupancy for each shell.

When an electron is removed from one of the inner shells (lower energy levels), an electron from an outer shell (higher energy level) can drop down to the inner shell and release energy as a photon in the process. Shells have well-defined energies, so only photons of some specific energies (and hence wavelengths) are observed for any particular element. Since these are characteristic of the atom, these are known as *characteristic radiation*, or characteristic x-rays when the photon is an x-ray.

Typically, characteristic x-rays may be suitable for external measurement if they are sufficiently energetic to penetrate a few centimeters of body tissue. While there is no precise energy cutoff point, 25 keV is a reasonable minimum for shallow organs such as the thyroid. For elements with $Z \geq 50$, the energy of K-x rays - photons emitted due to transitions from an outer shell to the K shell - exceeds 25 keV. The K-x rays of lighter elements and all L-x rays are of lower energy and generally are not suitable for measurements.

2.2.2 Auger Electrons

The Auger effect is a general phenomenon observed in many decay processes as an alternative to characteristic x-ray emission. In this effect, when an electron from an outer shell drops to an inner shell to fill a vacancy, the energy may be transferred to another electron, which may then have enough energy to escape the atom - be emitted. It is then known as an *Auger electron*.

Now we cover the various modes of radioactive decay.

2.2.3 β^- Emission Decay

In this process, a neutron in the nucleus transforms into a proton and an electron - the electron is what is known as the β^- particle. The reaction is represented as: $\mathrm{n} \longrightarrow \mathrm{p}^+ + \mathrm{e}^- + \bar{\nu} + \text{Energy}$ Where $\bar{\nu}$ is an anti-neutrino.

The nuclide changes as: ${}^{\mathrm{A}}_{\mathrm{Z}}\mathrm{X} \xrightarrow{\beta^-} {}^{\mathrm{A}}_{\mathrm{Z+1}}\mathrm{Y}$

Z changes, so the process is considered a transmutation of the element, whereas A does not, so it is an isobaric decay.

The energy released is distributed among the kinetic energy of the electron and the anti-neutrino. We refer to the total energy released as $E^{\max}$. The average energy of the electron (over many sample decays) is characteristic for a nuclide. Typically, $\langle E_\beta \rangle \approx (1/3)E^{\max}$.

Beta particles can only penetrate thin layers, so this kind of decay is not helpful for imaging applications.

β^-, γ Emission Decay

This is a special case of β^- Emission Decay where the duaghter nuclide is excited and decays further.

The nuclide changes as: ${}^{\mathrm{A}}_{\mathrm{Z}}\mathrm{X} \xrightarrow{\beta^-} {}^{\mathrm{A}}_{\mathrm{Z+1}}\mathrm{Y}^* \xrightarrow{\gamma} {}^{\mathrm{A}}_{\mathrm{Z+1}}\mathrm{Y}$

Unlike beta particles, the gamma rays can only have certain energies, since they are emitted by an electron falling from an outer to an inner shell.

Because γ rays are much more penetrating than β^- particles, they do not present some of the beforementioned measurement problems associated with β^- particles, and they are suitable for a wider variety of applications in nuclear medicine.

Isomeric Transition

Similar to β^-, γ Emission Decay, but an isomeric (metastable) state is formed after β^- decay instead of an excited state.

Internal Conversion

When an excited or meta-stable state de-excites, the energy may cause the ionisation of another electron instead of being released as a γ ray, which is then known as a conversion electron. The possible energies of this electron are a discrete set. This vacancy is filled by further de-excitations and may release further x-rays or Auger electrons.

2.2.4 Electron Capture Decay

Colloquially known as EC decay or inverse β^- decay, this involves an orbital electron combining with a proton to create a neutron. The reaction is represented as: $\mathrm{p}^+ + \mathrm{e}^- \longrightarrow \mathrm{n} + \nu + \mathrm{Energy}$ Where ν is a neutrino. The energy is distributed among the kinetic energy of the neutrino and the characteristic x-rays and Auger electrons created by the de-excitations that fill the vacancy.

The nuclide changes as: ${}^{\mathrm{A}}_{\mathrm{Z}}\mathrm{X} \xrightarrow{\mathrm{EC}} {}^{\mathrm{A}}_{\mathrm{Z}-1}\mathrm{Y}$

As with β^- decay, excited or metastable daughter nuclides can further release γ rays.

2.2.5 Positron (β^+) Decay

In this process, a proton decays to a neutron and the anti-particle of an electorn, the positron. The positron has the same mass as an electron and shares many other properties, but it has the opposite charge. The reaction is represented as: $\mathrm{p}^+ \longrightarrow \mathrm{n}^+\mathrm{e}^+ + \nu + \mathrm{Energy}$

Anti-matter annihilates with corresponding matter to create photons, so the emitted positron quickly finds an electron and undergoes annhilation. The rest-mass energy of both electrons and positrons is $0.511\,\mathrm{MeV}$, so annihilation releases two $0.511\,\mathrm{MeV}\gamma$ rays with nearly opposite momenta. Because photons of a particular energy have a fixed momentum, which is much larger than the small momentum of the positron, momentum conservation demands that their momenta be nearly opposite.

The nuclide changes as: ${}^{\mathrm{A}}_{\mathrm{Z}}\mathrm{X} \xrightarrow{\beta^+} {}^{\mathrm{A}}_{\mathrm{Z}-1}\mathrm{Y}$

Having two photons per event and a relationship between their directions

allows for better imaging using coincidence-counting techniques, which we focus on later.

Competitive β^+ and EC Decay

Since both these processes have the same initial and final states, they compete with each other. β^+ is more common among lighter elements, whereas in heavier elements the shell radii are smaller so EC decay becomes more common.

2.2.6 α Emission

In this process, the nucleus ejects an α particle, which is essentially a Helium nucleus. The nuclide changes as: ${}^{A}_{Z}X \xrightarrow{\alpha} {}^{A-2}_{Z-2}Y$

The resulting α particle is highly energetic and also somewhat dangerous, since it is considered a much higher radiation dose per particle. This process happens mainly in very heavy elements and is not very useful in nuclear medicine.

2.3 Image Quality

To be able to compare various approaches, we require parameters to characterise and measure image quality. Some of them are described in this section.

2.3.1 Spatial Resolution

Spatial resolution is, intuitively, the sharpness of the image. It depends on both the collimator's and detector's intrinsic resolution. Since collimators are often absent from PET systems, this can improve the resolution.

The intrinsic resolution becomes poor with decreasing Γ ray energy. In PET, the size of the individual detector elements determines the intrinsic resolution of the device.

Besides these, patient motion and other blurring factors can also limit the spatial resolution.

Methods to evaluate the spatial resolution

A subjective evaluation can be done by looking at the images of the organ phantoms. **Phantoms** are objects used as stand-ins for human tissues to test the working and quality of an imaging device.

Bar phantoms consist of strips of lead or tungsten of varying sizes. They are placed on the collimated detector and irradiated with uniform radiation - perhaps using a faraway point source. The spatial resolution is expressed as the smallest bar pattern visible on the image.

A more quantitative approach involves the usage of a point spread function (PSF) or a line spread function (LSF).

2.3.2 Contrast

Image contrast refers to differences in intensity in parts of the image corresponding to different levels of radioactive uptake in the patient. In nuclear medicine, a major component of image contrast is determined by the properties of the tracer. In general, it is desirable to use a tracer having the highest lesion-to-background uptake ratio.

Mathematically, the contrast is the ratio of intensity of an object of interest to the intensity in surrounding parts of the image. If R_o is the intensity measured from normal tissue and R_l from a lesion, then contrast is given by :

$$C_l = (R_l - R_o)/R_o = \Delta R_l/R_o \tag{2.1}$$

Contrast is majorly affected by additional background radiation generated by septal penetration, scattered radiation and radioactivity outside the object of interest (the latter being significant in planar imaging). *Septa* are the walls making up the collimator, and septal penetration occurs when they are not sufficiently thick.

2.3.3 Noise

Noise can be **random** or **structured**.

Random - Noise caused by random variations in counting rates, causes a mottled appearance in images.

Structured - Noise from deterministic accidental sources, such as uptake of the tracer by non-targeted tissues in the area of interest, system

artifacts due to broken or asymmetric detectors or reconstruction artifacts created by algorithms being used to reconstruct the image from measured data.

2.3.4 Contrast to Noise Ratio (CNR)

The CNR is another measure of image quality. To understand its definition, a few terms need to be introduced.

If a 2D image contains a circular lesion of Area A_l with a contrast C_l with a uniform background counting rates of R_0, then N_0, the number of counts recorded in a background area of same size, equals

$$N_0 = (R_0 \cdot d_l^2 \cdot t)/4 \tag{2.2}$$

The standard deviation of counts due to random statistical variations is $\sigma_{N_0} = \sqrt{N_0}$, and the fractional standard deviation of counts is $C_{noise} = \sigma_{N_0}/N_0$.

Then the CNR is defined as

$$\mathrm{CNR}_l = C_l/C_{noise} \tag{2.3}$$

To detect a lesion or other object in an image the observer must be able to distinguish between the lesion and noise-generated contrast patterns in background areas of the same size in the image. The **Rose Criterion**, derived from substantial research into the subject, is that an object's CNR must exceed $3 - 5$ to be detectable.

2.4 Tomographic Reconstruction

A fundamental challenge faced in imaging is that of the obtained images being 2D projections of 3D source distributions. A projection - the product of planar imaging - may have features of interest obscured by structures above and below. This can be overcome to some extent by creating views from multiple angles (e.g. posterior, anterior, lateral, and oblique views) and then comparing them mentally - but for more complicated structures it may be challenging to make sense of multiple images, and some features may be obscured from all views.

When more detail is required, a solution may be *tomographic imaging*, in which many 2D projections at various angles are taken and then used to mathematically reconstruct the 3D distribution, which is then viewed as a set of cross-sections.

We assume that we are imaging with a gamma camera fitted with parallel-hole collimators for single photon imaging. In the case of positron imaging, coincidence detection provides us with similar information, and the algorithms can be extended without too much effort. Furthermore, we reduce the system to that of a 1D camera imaging a 2D source distribution, assuming that the camera only recieves radiation from a thin slice perpendicular to the camera face due to the collimators. Each collimator defines a cylinder extending through it called the *line of response*, and we assume only the radiation inside that thin cylinder is measured by that collimator's hole - the measured counts are known as the *line integral* for the particular line of response. The *projection profile* consists of all such line integrals.

2.4.1 Radon Transform

There are various ways to obtain projections from multiple angles, e.g. rotating a single detector or having a stationary set of detectors at different angles. In either case, it is useful to record the data in the detector's reference frame. The Radon transform relates the source distribution in the $x-y$ plane and the measurements of an ideal detector.

Assume a detector with its normal making an angle of θ with the y-axis. We measure distance parallel to the detector face on a new r-axis, which will also be at an angle θ with the x-axis. We measure distance along the normal to the detector face with the new s-axis. Then the transformation from (x, y) to (r, s) coordinates is:

$$r = x\cos\theta + y\sin\theta \tag{2.4}$$

$$s = y\cos\theta - x\sin\theta \tag{2.5}$$

Finally, what we desire is the projection information dependent on the r, θ coordinates. Each θ denotes the detector at different angles, and r parametrises the 1D projection obtained by each detector.

Let the source distribution be $f(x, y)$. The projection at a particular θ is

given by the **Radon Transform**,

$$\rho(r,\theta) = \int_{-\infty}^{\infty} f(x(r,s), y(r,s))ds \tag{2.6}$$

$$x(r,s) = r\cos\theta - s\sin\theta \tag{2.7}$$

$$y(r,s) = s\cos\theta + r\sin\theta \tag{2.8}$$

This is a continuous function - however, practically, we only take a finite amount of projections and have a finite step-size for r, so we obtain a discrete $\rho(r,\theta_i)$. This is often represented as a matrix for further calculations.

2.4.2 Backprojection

Backprojection is the simplest algorithm to go from a projection matrix to an estimate of the source distribution.

For each projection profile $\rho(r,\theta_i)$, we distribute the profile uniformly over the $x-y$ plane (technically, some finite subset of the $x-y$ plane).This step is also called *backprojection*. As an example, if $\rho(r,0^\circ)$ equals 1 at $r=0$ and 0 elsewhere, the backprojection will give a grid in the $x-y$ plane consisting of 1s along the line $x=0$ and 0s everywhere else.

The next step is to take the average of all these backprojections (essentially functions in the $x-y$ plane). This gives an approximation to the source distribution.

Mathematically we can write both steps in one (For N projections):

$$f'(x,y) = \frac{1}{N}\sum_{i=1}^{N} \rho(x\cos\theta_i + y\sin\theta_i, \theta_i) \tag{2.9}$$

$1/r$ Blurring

With too few projection angles, this algorithm may lead to spoke-like artifacts. These are suppressed with more angles, but there is always some blurring no matter how many angles are used. Even in the limit of infinite projection angles and infinite detector resolution, the reconstructed image is

blurred, as given by the following relation (where $*$ denotes convolution):

$$f'(x,y) = f(x,y) * \frac{1}{r} \tag{2.10}$$

$$r = \sqrt{x^2 + y^2} \tag{2.11}$$

Intuitively, this means that a point source leads to an image which has a $1/r$ distribution about the point source. This behaviour is known as $1/r$ *blurring*.

2.4.3 Fourier Transform Reconstruction

One approach to avoid $1/r$ blurring is known as Fourier Transform Reconstruction. The Fourier transform takes a function from its input space to that input's frequency space, giving the amplitudes of various frequency components in the function. The continuous and discrete Fourier transforms respectively are given below.

$$\tilde{f}(k) = \int_{\mathbb{R}} f(x) e^{-ikx} dx \tag{2.12}$$

$$\tilde{f}(k_j) = \sum_{i=1}^{n} f(x_i) e^{-ik_j x_i} \tag{2.13}$$

$$\text{Both of which may be written as } \tilde{f}(k) = \mathcal{F}(f(x)) \tag{2.14}$$

To utilise this for reconstruction purposes, we need the Fourier slice theorem.

Fourier Slice Theorem

Take the projection of a 2-D object along a projection angle θ. Its 1D fourier transform is equal to the 1-D slice of the 2-D fourier transform of the original object taken along a line through the origin at an angle θ with the k_x axis (the line is in k-space).

Hence, the total 2-D fourier transform of the original object is obtained by combining the projections along all angles. Then the inverse fourier transform allows us to get back the original object.

$$\tilde{\rho}(k_r, \theta) = \mathcal{F}(\rho(k, \theta)) \tag{2.15}$$
$$k'_x = k_r \cos\theta \tag{2.16}$$
$$k'_y = k_r \sin\theta \tag{2.17}$$
$$\therefore \tilde{f}(k_x, k_y) = \tilde{\rho}(\sqrt{k_x^2 + k_y^2}, \arctan k_y/k_x) \tag{2.18}$$
$$f(x, y) = \mathcal{F}^{-1}(\tilde{f}(k_x, k_y)) \tag{2.19}$$

Practically, discrete transforms are used, and so before the last step of taking the inverse fourier transformm, which requires a grid of values in k_x-k_y-space, an interpolation step must occur to obtain that grid, since the distribution in k_x-k_y-space obtained from the Fourier Slice Theorem is much more dense closer to the origin when using discrete transforms, and not grid-like as we require.

This over-representation of data near the origin in the k_x-k_y-space is intuitively why the FT Reconstruction method does not lead to $1/r$ blurring. In fact, with measurements at infinite projection angles and detectors with infinitesimal resolutions, this method would give back the exact source distribution. But it is not without flaw and may create artifacts in the image.

2.4.4 Filtered Backprojection

This technique uses fourier transforms to suppress lower spatial frequencies (and amplify higher ones) before backprojection is done. It is effective in eliminating $1/r$ blurring. The implementation is quite simple:

$$\tilde{\rho}(k_r, \theta) = \mathcal{F}(\rho(r, \theta)) \tag{2.20}$$
$$\tilde{\rho}'(k_r, \theta) = H(k_r)\rho(k_r, \theta) \tag{2.21}$$
$$\rho'(r, \theta) = \mathcal{F}^{-1}\tilde{\rho}'(k_r, \theta)f(x, y) = \frac{1}{n}\sum_{i=1}^{n} \rho'(x\cos\theta_i + y\sin\theta_i, \theta_i) \tag{2.22}$$

Where $H(k)$ is called the reconstruction filter in frequency space. There are various types used, but all have the common feature of being increasing functions of k. The most basic is the Ramp Filter, which linearly amplifies

$\rho(k_r, \theta)$ by $|k_r|$. Because of the amplification of higher frequencies, high-frequency noise is also amplified and the signal-to-noise ratio of the image degrades. To combat this, other commonly-used filters smoothen out or drop off at high frequencies after peaking.

$$\text{Ramp Filter} : H(k) = |k| \tag{2.23}$$

$$\text{Shepp-Logan Filter} : H(k) = \frac{2k_{\text{cut-off}}}{\pi} \sin\left(\frac{\pi|k|}{2k_{\text{cut-off}}}\right) \tag{2.24}$$

$$\text{Hann Filter} : H(k) = 0.5|k| \left[1 + \cos\left(\frac{\pi k}{k_{\text{cut-off}}}\right)\right] \tag{2.25}$$

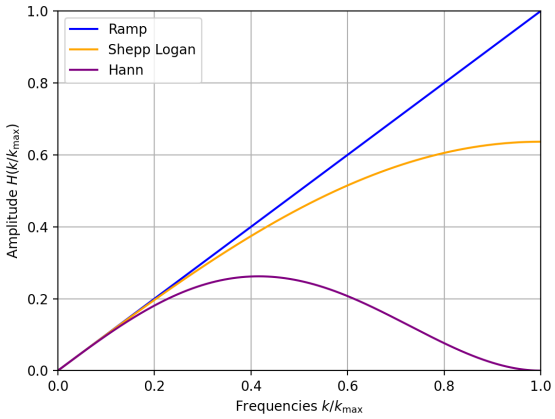

Figure 2.1: Types of frequency filters. $k_{\text{cut-off}}$ is optimised for size of system and noise.

2.4.5 Iterative Reconstruction

Iterative Reconstruction Algorithms seek to improve upon the defects of the previously-described algorithms, especially the various artifacts they have tendencies towards creating. The trade-off is computation time - however, with increases in processing power they have become viable.

An iterative algorithm starts with some assumption of the image, then calculates its projection and compares that with the physically obtained projection data. The difference in these two is used to update the assumption

of the image, and this process repeats until the differences reach some sufficiently small values. While this seems simple on the surface, the complexity lies in the approaches to obtain the difference (called the *cost function*) and update the assumption (called the *update function*).

ML-EM Algorithm

The Maximum-Likelihood Expectation-Maximisation Algorithm is one of the simpler iterative algorithms, and is briefly presented here.

Given any image, label all its pixels with the subscript i, and all elements of the projection with the subscript j. Then define f_i as the intensity of the i^{th} pixel, p_j the masured intensity of the j^{th} projection element, and M_{ij} the probability that radiation emitted from i will be detected by j. Then:

$$p_j = \sum_i M_{ij} f_i \tag{2.26}$$

The cost and update functions are then combined into one as a function to obtain the next image f_i^{n+1} from the previous image f_i^n as (where p_j^n is obtained from f_i^n):

$$f_i^{n+1} = \frac{f_i^n}{\sum_j M_{ij}} \sum_k \frac{M_{ik} p_k^n}{\sum_l M_{lk} f_l^n} \tag{2.27}$$

2.5 Positron Emission Tomography

As covered in subsection 2.2.5, when a radionuclide decays by emitting a positron, the positron annihilates with a nearby electron to create two $0.511\,\text{MeV}\gamma$ rays with nearly opposite momenta. Because photons of a particular energy have a fixed momentum, which is much larger than the small momentum of the positron, momentum conservation demands that their momenta be nearly opposite.

Detectors designed for SPECT (Single Photon Emission Computed Tomography) are inefficient at the high energy level of annihilation photons and also do not take advantage of the opposite momenta of the photons. Special systems have been designed to take advantage of these and are known as PET scanners. They detect gamma rays and try to accurately pair them as annhilation photons from the same source. A pair is known as a coincidence event.

2.5.1 Annihilation Coincidence Detection

Annihilation photons are detected nearly simultaneously in different sections of the detector system. If they can be confidently paired, it can be determined that their source lies on the line between the two points of detection. Hence, localisation can be achieved without requiring absorptive collimators, which lead to significant ineffiency - this feature is sometimes called *electronic collimation*.

Detectors have finite timing resolution, and so a sufficiently large *coincidence timing window* must be specified, such that photons detected within this window of each other are paired. Typically, this window is $6-12ns$ long.

PET also has other possible issues, some of which are briefly discussed below:

Scattering is when a photon interacts with matter and changes its trajectory - this can lead to inacurate localisation and hence noise.

Random coincidence is when wrong sets of photons are paired up. These are frequent enough to warrant consideration, especially in cases when radioactivity is present nearby but outside the volume being scanned, such as if large amounts of activity is excreted into the bladder while imaging the abdomen.

Positron travel is the distance the positron moves before annhilating. It has an effect on the spatial resolution given by R_{trav}

Non-colinearity is the fact that the momenta of the photons are nearly opposite, but not precisely. The angular deviation has a gaussian distribution, and the effect on spacial resolution is given by $R_{\text{ang}} = 0.0022D$, where D is the distance between detectors.

Assuming the detector's spatial resolution to be given by R_0, the net spatial resolution is calculated as

$$R = \sqrt{R_0^2 + R_{\text{trav}}^2 + R_{\text{ang}}^2} \tag{2.28}$$

Because the spatial resolution is expressed as a Full-Width by Half Maximum of a point-source response profile, and this is how FWHMs of different gaussian distributions combine.

2.5.2 Time-of-Flight PET

It is theroetically possible to determine the location along a line between two ACD detectors at which the annihilation photons originated using the difference in time of detection. This technique, which would allow the construction of tomographic images without reconstruction algorithms, is called time-of-flight PET. If the difference in the arrival times of the photons is Δt, the location of the annihilation event, with respect to the midpoint between the two detectors, is given by (c being the speed of light) :

$$\Delta d = \frac{1}{2}\Delta t \cdot c \tag{2.29}$$

The limiting factor in utilising this technique is the timing resolution of scintillators. With the fastest available scintillators and careful design of the electronics, it is possible to achieve timing accuracy of the order of a few hundred picoseconds. While this only allows localisation to within a few centimeters, this technique leads to higher signal-to-noise ratios than images reconstructed without using time-of-flight information.

2.5.3 Polarisation Correlation

To create accurate images using PET scans, it is vital to correctly identify pairs of annhilation photons, also known as *true coincidence events*. In existing systems, various techniques are used to identify false coincidence events, but they generally discard any such events, leading to signal and contrast loss.

False coincidences may be caused by

Randoms which consist of detecting photons of multiple annhilations in the same time window.

Multiples which consist of more than two photons being detected in the same window.

Scattering which does not lead to false events, but an incorrect localisation of the event.

An exploitable property of an annhilation photon pair is that their polarisations are correlated, as seen in Fig 2.2. This is caused by the conservation

of angular momentum during annhilation - before annhilation, the positron generally reaches a short-lived zero momentum bound state with an electron, so the angular momentum is insignificant prior to photon creation, and so must be after as well.

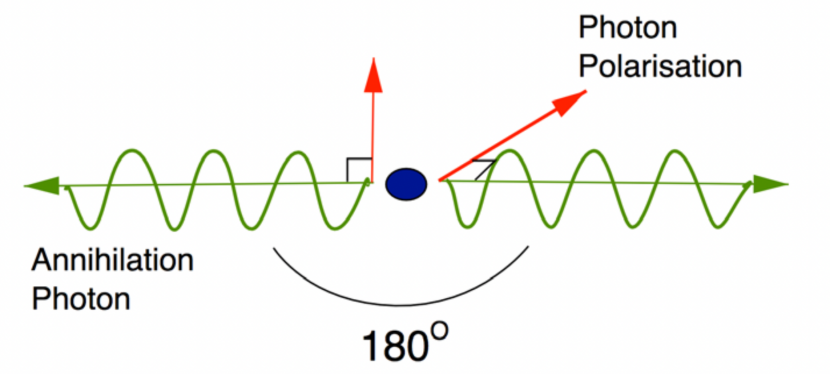

Figure 2.2: The polarisations of the two emitted photons are orthogonal to each other. *Image Credits: [1]*

This property can be used to identify true coincidences by utilising a Compton camera. A Compton camera exploits compton scattering to deduce the photon's trajectory. A linearly polarised photon which undergoes a Compton interaction will scatter in directions preferentially perpendicular to the initial polarisation vector. Thus a pair of annhilation photons will have an angular correlation measurable by a Compton camera, which can be used to obtain true coincidences from both Randoms and Multiples.

Chapter 3

Simulation

3.1 GATE

To simulate imaging processes and test various approaches and reconstruction algorithms, I am using GATE, a Monte-Carlo simulation toolkit for medical physics applications. The name is an acronym for "GEANT4 Application for Tomographic Emission", since GATE is based on GEANT4, a toolkit for the simulation of the passage of particles through matter.

3.1.1 Language

GATE incorporates a simple high-level scripting language, so no C++ programming is required for working with GATE. This section leads the reader through an overview of a macro for an imaging simulation. The full macro, which is also used to obtain the results displayed later, is attached in Appendix A.

The steps to set-up an imaging simulation are:

1. Define the scanner geometry
2. Define the phantom geometry
3. Set up the physics processes
4. Initialize the simulation

5. Set up the detector model
6. Define the sources
7. Specify the data output format
8. Start the acquisition

Prior to other steps, it is necessary to define the location of a database of materials if you wish to define the material of various objects in your simulation.

```
/gate/geometry/setMaterialDatabase GateMaterials.db
```

Scanner Geometry

All geometries in the simulation are defined using *volumes*. Volumes are stored in a tree structure - any new volume is defined as the daughter of a pre-defined volume. There is a pre-existing volume known as `world`, the dimensions of which can be set as

```
/gate/world/geometry/setXLength 50 cm
```

A daughter volume is defined and its shape is fixed as follows

```
/gate/world/daughters/name cylindricalPET
/gate/world/daughters/insert cylinder
```

We can also set the position, size, material or colour of any volume with commands of the following form:

```
/gate/volume/placement/setTranslation 20.0 0.0 0.0 cm
/gate/volume/geometry/setRmax 40 cm # For cylinder
/gate/volume/geometry/setXLength 10 cm # For box
/gate/volume/setMaterial Water
/gate/volume/vis/setColor red
```

Generally, small detector units are defined, and then a *repeater* is used to have these volumes duplicate to create the full detector set-up. Below is an example of a cubic repeater, which creates a grid of duplicates of the volume.

```
/gate/Crystal_unit/repeaters/insert cubicArray
/gate/Crystal_unit/cubicArray/setRepeatNumberX 9
/gate/Crystal_unit/cubicArray/setRepeatNumberY 1
```

```
/gate/Crystal_unit/cubicArray/setRepeatNumberZ 13
/gate/Crystal_unit/cubicArray/setRepeatVector 1 0 1 cm
```

Then these volumes must be associated with various levels of the predefined detector system, after which they can be defined to be *sensitive* - interactions with photons are only stored for volumes attached to sensitive detectors.

```
# Attach volumes to system levels
/gate/systems/cylindricalPET/rsector/attach PET_unit
/gate/systems/cylindricalPET/module/attach Crystal_unit
# Make sensitive
/gate/Crystal_unit/attachCrystalSD vglue 1 cm
```

Phantom Geometry

The phantom is defined as a volume similarly to scanner, with the exception that the command to make a phantom volume sensitive differs slightly:

```
/gate/body_phantom/attachPhantomSD
```

The commands to define certain parts of the phantom to be radioactive are part of 3.1.1.

Physics Processes

The interaction processes between particles need to be specified as well, in a *physics list*. For most purposes, however, one of the physics lists provided with the installation will suffice. If not, further customisation is possible after using a given physics list. The following command adds `egammaStandardPhys.mac`, a physics list for photons, electrons and positrons with standard processes included, to the simulation.

```
/gate/physics/addPhysicsList emstandard_opt3
```

Initialise

The above steps correspond to the pre-initialisation mode of GEANT4. Once those are complete, the simulation should be initialised with the following command:

```
/gate/run/initialize
```

This initialization triggers the calculation of the cross section tables. After this step, the physics list cannot be modified any more and new volumes cannot be inserted into the geometry.

Digitizer

By default GATE stores and outputs *hits*, which are interactions of a particle with a sensitive region. But these are not what an actual detector would provide. The role of the **digitizer** is to build, from the hit information, the physical observables a detector will measure, which include energy, position, and time of detection for each particle. In addition, the digitizer must implement the required logic to simulate coincidences during PET simulations.

The digitizer can be modelled as a series of signal processers, and modules can be added to account for blurring, energy thresholds, and other artifacts of the system being simulated. The output of this signal-processing is data known as *Singles*, which correspond to the physical observables of a detector response to a particle.

For example, this command collects the hits generated in each elementary volume:

```
/gate/digitizer/Singles/insert adder
```

This command introduces blurring at non-reference energies of the detector:

```
/gate/digitizer/Singles/insert                     blurring
/gate/digitizer/Singles/blurring/setResolution     0.40
/gate/digitizer/Singles/blurring/setEnergyOfReference 511. keV
```

And this command implements a coincidence sorter, by instructing that singles within $10ns$ of each other should be regarded as a coincidence:

```
/gate/digitizer/Coincidences/setWindow          10 ns
```

Sources

A source is a volume which emits some particles. The following commands add a $0.1MBq$ source which generates two gamma rays of $0.511MeV$ and opposite momenta simultaneously.

```
/gate/source/addSource twogamma
/gate/source/twogamma/setActivity 100000. becquerel
/gate/source/twogamma/setType backtoback
/gate/source/twogamma/gps/particle gamma
/gate/source/twogamma/gps/ene/type Mono
/gate/source/twogamma/gps/ene/mono 0.511 MeV
```

Further attributes of the source, such as the position, shape, angular distribution of emission, etc can also be defined.

Output Format

A hit is a snapshot of the physical interaction of a track within a sensitive region of a detector. The information given by a hit is

1. Position and time of the step
2. Momentum and energy of the track
3. Energy deposition of the step
4. Interaction type of the hit
5. Volume name containing the hit

The digitizer then converts this data into Singles and Coincidences. At this stage we can define in what file format we want the output, as well as what data we want in the output.

By default, GATE stores the output in ASCII and ROOT[2] formats. We will prefer to use the ROOT format for visualisation and further processing (including reconstruction of the phantom).

For example, setting the file format to root:

```
/gate/output/root/enable
/gate/output/root/setFileName output/pet
```

Instructing that Singles and Coincidences be stores, but not Hits:

```
/gate/output/root/setRootHitFlag          0
/gate/output/root/setRootSinglesFlag      1
/gate/output/root/setRootCoincidencesFlag 1
```

Acquisition

GATE allows for motion of the detector and the phantom - however, this is implemented by having time periods with no motion when particle transport and data collection is simulated, between which the geometry is updated with movements. This time period can be defined along with the start and stop time of the data collection. If no motion has been programmed, the time slice can be arbitrary:

```
/gate/application/setTimeStart 0 s
/gate/application/setTimeSlice 20 s
/gate/application/setTimeStop  20 s
```

Furthermore, it is possible to select a randomness engine and a seed for the engine in this step.

```
/gate/random/setEngineName MersenneTwister
/gate/random/setEngineSeed 123456789
```

Finally, the following command begins the simulation:

```
/gate/application/startDAQ
```

Visualisation

It is possible to attach visualisation commands to volumes and hence generate an image of the system being simulated. The image obtained from the code in Appendix A is given in Fig 3.1.

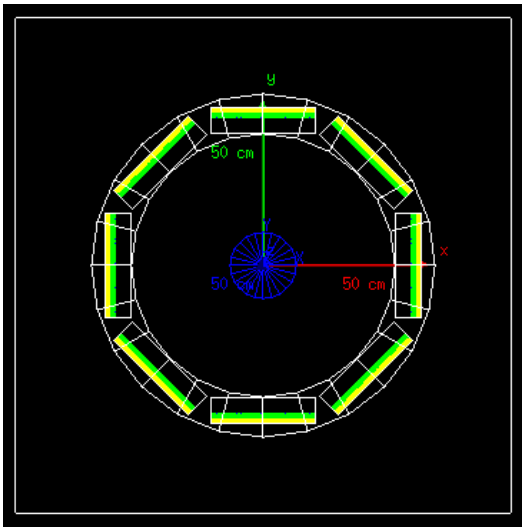

Figure 3.1: The PET scanner configuration encoded in Appendix A, visualised

3.1.2 Results

On running the code in Appendix A, a ROOT file is obtained as the output, containing the data in List Mode Format, with different folders for Hits, Singles and Coincidences. ROOT includes a commmand line interface that can be accessed with the command `root` on the terminal. Via the ROOT command line, one can load the output file and visualise the data using the following commands:

```
root [0] .L Output/pet.root
root [1] TBrowser b
```

Some relevent visualisations are given in Figs 3.2, 3.3, 3.4.

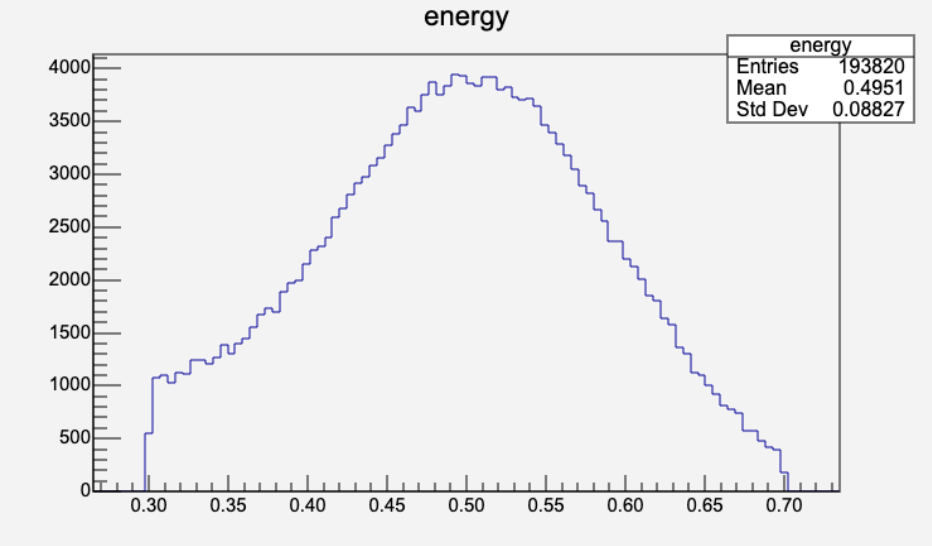

Figure 3.2: The energy histogram of the detected photons, from the Singles folder. Peaks at 511 keV. Units are MeV.

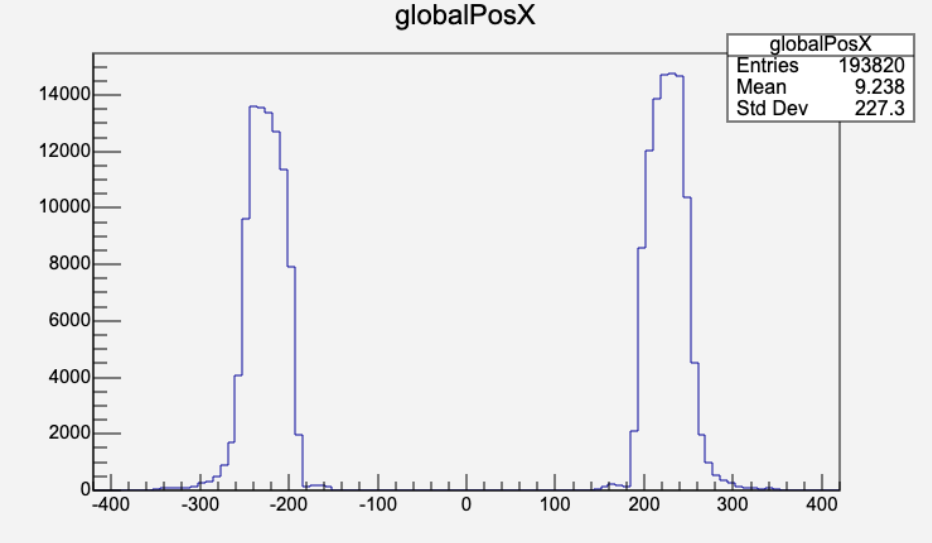

Figure 3.3: The histogram of x-coordinates of the positions where the photons were **detected**, from the **Singles** folder. Peaks can be seen at the locations of the detectors. This functions as a sanity check. Units are mm.

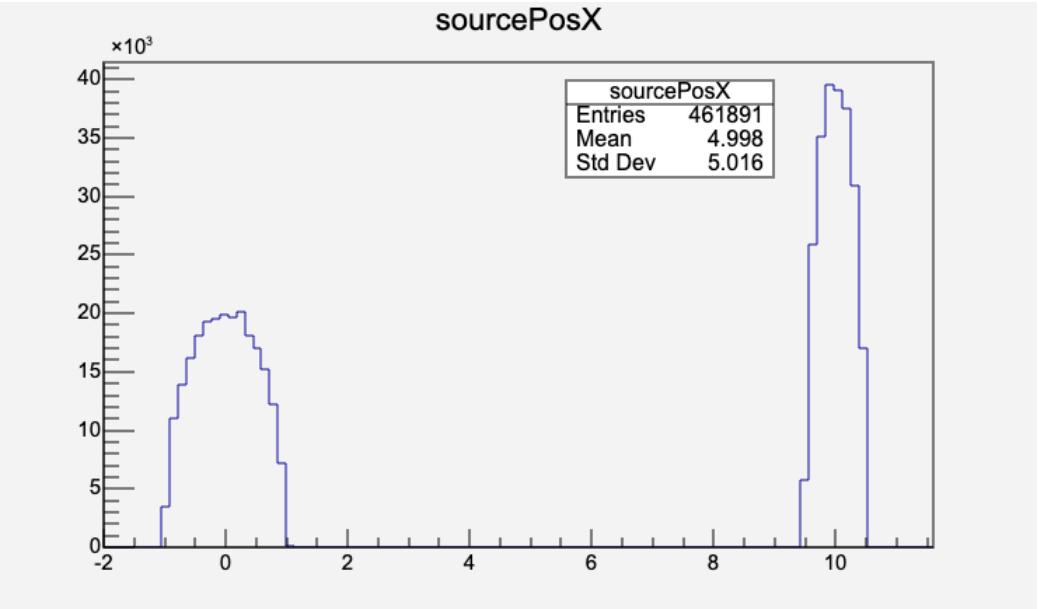

Figure 3.4: The histogram of x-coordinates of the positions where the photons were **created**, from the **Hits** folder. Peaks can be seen at the locations of the sources. Since both sources have the same activity, the smaller source has a higher intensity. Units are mm.

Appendix A

GATE Macro Code

```
# Geometry
# Material Database
/gate/geometry/setMaterialDatabase GateMaterials.db

# World
/gate/world/geometry/setXLength 50 cm
# x is the direction of the phantom's orientation
# The detector is in the y-z plane
/gate/world/geometry/setYLength 50 cm
/gate/world/geometry/setZLength 50 cm
/gate/world/setMaterial Air
/gate/world/vis/forceWireframe

# Cylindrical Scanner
/gate/world/daughters/name cylindricalPET
/gate/world/daughters/insert cylinder
/gate/cylindricalPET/geometry/setRmax 40 cm
/gate/cylindricalPET/geometry/setRmin 30 cm
/gate/cylindricalPET/geometry/setHeight 10 cm
/gate/cylindricalPET/setMaterial Water
/gate/cylindricalPET/vis/setColor blue
/gate/cylindricalPET/vis/forceWireframe

```

```
# Head
/gate/cylindricalPET/daughters/name PET_unit
/gate/cylindricalPET/daughters/insert box
/gate/PET_unit/placement/setTranslation 35.0 0.0 0.0 cm
/gate/PET_unit/geometry/setXLength 10 cm
/gate/PET_unit/geometry/setYLength 10 cm
/gate/PET_unit/geometry/setZLength 14 cm
/gate/PET_unit/setMaterial Water
/gate/PET_unit/vis/setColor yellow
/gate/PET_unit/vis/forceWireframe

# Crystal
/gate/PET_unit/daughters/name Crystal_unit
/gate/PET_unit/daughters/insert box
/gate/Crystal_unit/placement/setTranslation 0.0 0.0 0.0 cm
/gate/Crystal_unit/geometry/setXLength 1 cm
/gate/Crystal_unit/geometry/setYLength 8 cm
/gate/Crystal_unit/geometry/setZLength 1 cm
/gate/Crystal_unit/setMaterial LSO
/gate/Crystal_unit/vis/setColor red
/gate/Crystal_unit/vis/forceWireframe

# Repeat Crystal
/gate/Crystal_unit/repeaters/insert cubicArray
/gate/Crystal_unit/cubicArray/setRepeatNumberX 9
/gate/Crystal_unit/cubicArray/setRepeatNumberY 1
/gate/Crystal_unit/cubicArray/setRepeatNumberZ 13
/gate/Crystal_unit/cubicArray/setRepeatVector 1 0 1 cm

# Repeat block
/gate/PET_unit/repeaters/insert ring
/gate/PET_unit/ring/setRepeatNumber 16

# Attach volumes
/gate/systems/cylindricalPET/rsector/attach PET_unit
/gate/systems/cylindricalPET/module/attach Crystal_unit

# Sensitive detector
```

```
/gate/Crystal_unit/attachCrystalSD vglue 1 cm

# Phantom
/gate/world/daughters/name body_phantom
/gate/world/daughters/insert cylinder
/gate/body_phantom/geometry/setRmax 1 cm
/gate/body_phantom/geometry/setHeight 50 mm
/gate/body_phantom/setMaterial Water
/gate/body_phantom/vis/setColor grey

# Sensitive phantom
/gate/body_phantom/attachPhantomSD

# Physics
/gate/physics/addPhysicsList emstandard_opt3

/gate/physics/Gamma/SetCutInRegion      world 1 m
/gate/physics/Electron/SetCutInRegion   world 1 m
/gate/physics/Positron/SetCutInRegion   world 1 m

/gate/physics/Gamma/SetCutInRegion      Crystal_unit 1 mm
/gate/physics/Electron/SetCutInRegion   Crystal_unit 1 mm
/gate/physics/Positron/SetCutInRegion   Crystal_unit 1 mm

/gate/physics/Gamma/SetCutInRegion      body_phantom 1 mm
/gate/physics/Electron/SetCutInRegion   body_phantom 1 mm
/gate/physics/Positron/SetCutInRegion   body_phantom 1 mm

# Initialisation
/gate/run/initialize
/gate/physics/displayCuts

# Digitiser
/gate/digitizer/Singles/insert adder
/gate/digitizer/Singles/insert readout
/gate/digitizer/Singles/readout/setDepth 1

/gate/digitizer/Singles/insert                          blurring
```

```
/gate/digitizer/Singles/blurring/setResolution        0.40
/gate/digitizer/Singles/blurring/setEnergyOfReference 511. keV

/gate/digitizer/Singles/insert                        thresholder
/gate/digitizer/Singles/thresholder/setThreshold      300. keV
/gate/digitizer/Singles/insert                        upholder
/gate/digitizer/Singles/upholder/setUphold            700. keV

/gate/digitizer/Coincidences/setWindow          10 ns
/gate/digitizer/Coincidences/MultiplesPolicy    takeWinnerOfGoods

# Visualisation
/vis/open                     OGLIQt
/vis/drawVolume
/vis/viewer/flush
/tracking/storeTrajectory     1
/vis/scene/add/trajectories
/vis/scene/endOfEventAction   accumulate

/vis/scene/add/axes            0 0 0 500 mm
/vis/scene/add/text            10 0 0 cm  20 0 0   X
/vis/scene/add/text            0 10 0 cm  20 0 0   Y
/vis/scene/add/text            0 0 10 cm  20 0 0   Z

/vis/viewer/set/auxiliaryEdge  true

# Source
/gate/source/addSource twogamma1
/gate/source/twogamma1/setActivity 100000. becquerel
/gate/source/twogamma1/setType backtoback

/gate/source/twogamma1/gps/pos/centre 0. 0. 0. cm

/gate/source/twogamma1/gps/particle gamma
/gate/source/twogamma1/gps/ene/type Mono
/gate/source/twogamma1/gps/ene/mono 0.511 MeV

/gate/source/twogamma1/gps/pos/type Volume
```

```
138
139 /gate/source/twogamma1/gps/pos/shape Cylinder
140 /gate/source/twogamma1/gps/pos/radius 1 mm
141 /gate/source/twogamma1/gps/pos/halfz 25 mm
142
143 /gate/source/twogamma1/gps/ang/type iso
144
145 /gate/source/twogamma1/gps/ang/mintheta 0. deg
146 /gate/source/twogamma1/gps/ang/maxtheta 180. deg
147 /gate/source/twogamma1/gps/ang/minphi 0. deg
148 /gate/source/twogamma1/gps/ang/maxphi 360. deg
149
150 /gate/source/addSource twogamma2
151 /gate/source/twogamma2/setActivity 100000. becquerel
152 /gate/source/twogamma2/setType backtoback
153
154 /gate/source/twogamma2/gps/pos/centre 10. 0. 0. mm
155
156 /gate/source/twogamma2/gps/particle gamma
157 /gate/source/twogamma2/gps/ene/type Mono
158 /gate/source/twogamma2/gps/ene/mono 0.511 MeV
159
160 /gate/source/twogamma2/gps/pos/type Volume
161
162 /gate/source/twogamma2/gps/pos/shape Cylinder
163 /gate/source/twogamma2/gps/pos/radius 0.5 mm
164 /gate/source/twogamma2/gps/pos/halfz 25 mm
165
166 /gate/source/twogamma2/gps/ang/type iso
167
168 /gate/source/twogamma2/gps/ang/mintheta 0. deg
169 /gate/source/twogamma2/gps/ang/maxtheta 180. deg
170 /gate/source/twogamma2/gps/ang/minphi 0. deg
171 /gate/source/twogamma2/gps/ang/maxphi 360. deg
172 /gate/source/list
173
174 /gate/source/list
175
```

```
176 # Output
177 /gate/output/root/enable
178 /gate/output/root/setFileName output/pet
179
180 /gate/output/root/setRootHitFlag          1
181 /gate/output/root/setRootSinglesFlag      1
182 /gate/output/root/setRootCoincidencesFlag 1
183 /gate/output/root/setRootNtupleFlag       0
184
185 # Randomness Generator
186 /gate/random/setEngineName MersenneTwister
187 /gate/random/setEngineSeed auto
188
189 # Start acquisition
190 /gate/application/setTimeStart 0 s
191 /gate/application/setTimeSlice 10 s
192 /gate/application/setTimeStop  20 s
193 /gate/application/startDAQ
```

Bibliography

[1] A L McNamara et al. "Towards optimal imaging with PET: an in silico feasibility study". In: *Physics in Medicine and Biology* (Apr. 2014). URL: https://iopscience.iop.org/article/10.1088/0031-9155/59/24/7587.

[2] *ROOT*. July 2022. URL: https://root.cern/.

[3] James A. Sorenson Simon R. Cherry and Michael E. Phelps. *Physics in Nuclear Medicine*. 4th ed. Elsevier Health Sciences, Apr. 2012.